Reshaping light: reconfigurable photonics enabled by broadband low-loss optical phase change materials

PROCEEDINGS OF SPIE

SPIEDigitalLibrary.org/conference-proceedings-of-spie

Reshaping light: reconfigurable photonics enabled by broadband low-loss optical phase change materials

Zhang, Yifei, Chou, Jeffrey, Shalaginov, Mikhail, Rios, Carlos, Roberts, Christopher, et al.

Yifei Zhang, Jeffrey B. Chou, Mikhail Shalaginov, Carlos Rios, Christopher Roberts, Paul Robinson, Bridget Bohlin, Qingyang Du, Qihang Zhang, Junying Li, Myungkoo Kang, Claudia Gonçalves, Kathleen Richardson, Tian Gu, Vladimir Liberman, Juejun Hu, "Reshaping light: reconfigurable photonics enabled by broadband low-loss optical phase change materials," Proc. SPIE 10982, Micro- and Nanotechnology Sensors, Systems, and Applications XI, 109820Q (13 May 2019); doi: 10.1117/12.2513385

SPIE.

Event: SPIE Defense + Commercial Sensing, 2019, Baltimore, Maryland, United States

Reshaping Light: Reconfigurable Photonics Enabled by Broadband Low-loss Optical Phase Change Materials

Yifei Zhang[1], Jeffrey B. Chou[2], Mikhail Shalaginov[1], Carlos Ríos[1], Christopher Roberts[2], Paul Robinson[2], Bridget Bohlin[2], Qingyang Du[1], Qihang Zhang[1], Junying Li[1], Myungkoo Kang[3], Claudia Gonçalves[3], Kathleen Richardson[3], Tian Gu[1], Vladimir Liberman[2], Juejun Hu[1]

[1]Department of Materials Science and Engineering, Massachusetts Institute of Technology, Cambridge, MA, USA
[2]Lincoln Laboratory, Massachusetts Institute of Technology Lexington, Massachusetts, USA
[3]College of Optics and Photonics, University of Central Florida, Orlando, Florida, USA

ABSTRACT

Optical phase change materials (O-PCMs) are a unique class of materials which exhibit extraordinarily large optical property change (e.g. refractive index change > 1) when undergoing a solid-state phase transition. Traditional O-PCMs suffer from large optical losses even in their dielectric states, which fundamentally limits the performance of optical devices based on the materials. To resolve the issue, we have recently demonstrated a new O-PCM Ge-Sb-Se-Te (GSST) with broadband low loss characteristics. In this talk, we will review an array of reconfigurable photonic devices enabled by the low-loss O-PCM, including nonvolatile waveguide switches with unprecedented low-loss and high-contrast performance, free-space light modulators, bi-stable reconfigurable metasurfaces, and transient couplers facilitating wafer-scale device probing and characterizations.

Keywords: Optical phase change materials, reconfigurable photonics, integrated photonics, metasurfaces

1. BROADBAND LOW-LOSS OPTICAL PHASE CHANGE MATERIALS

Chalcogenide optical phase change materials, such as Ge-Sb-Te (GST) compounds, have been exploited for a plethora of emerging optical applications including optical switching, photonic memories, reconfigurable metasurface, and non-volatile display[1-5].These traditional phase change materials, however, generally suffer from large optical losses even in their dielectric states. For instance, the archetypal ChA phase change material GST is optically absorbing at the telecommunication bands due to its small bandgap and the resulting interband absorption, whereas its crystalline form is plagued by high free carrier absorption (FCA) in the mid-wave and long-wave infrared (LWIR) (Fig. 1a). The large optical losses fundamentally limit the performance of photonic devices based on traditional O-PCMs. We define the optical figure-of-merit (FOM) for O-PCMs as: FOM = $\Delta n/k$, where Δn is the index change upon phase transition and k denotes the extinction coefficient. It can be directly shown that this FOM dictates the attainable insertion loss and contrast ratio of tunable optical devices based on O-PCMs[6]. Current O-PCMs solutions suffer from poor FOM's – mostly in the order of unity. This imposes a major hurdle towards their optical applications.

*hujuejun@mit.edu; phone 1-302-766-3083

This material is based upon work supported by the Under Secretary of Defense for Research and Engineering under Air Force Contract No. FA8702-15-D-0001. Any opinions, findings, conclusions or recommendations expressed in this material are those of the author(s) and do not necessarily reflect the views of the Under Secretary of Defense for Research and Engineering.

Micro- and Nanotechnology Sensors, Systems, and Applications XI, edited by Thomas George, M. Saif Islam, Proc. of SPIE Vol. 10982, 109820Q · © 2019 SPIE
CCC code: 0277-786X/19/$18 · doi: 10.1117/12.2513385

Besides the low material FOM, limited switching volume also poses a challenge for traditional O-PCMs. As an example, the poor amorphous phase stability of $Ge_2Sb_2Te_5$ (aka GST-225) requires a high cooling rate in the order of 10^{10} °C/s to ensure full re-amorphization during melt quenching[7]. Combined with their low thermal conductivity[8], it stipulates a film thickness of around 150 nm or even less if complete and reversible switching is needed. Although it is not an issue for today's electronic memory applications, it constrains optical device designs to thin film approaches.

This material is based upon work supported by the Under Secretary of Defense for Research and Engineering under Air Force Contract No. FA8702-15-D-0001. Any opinions, findings, conclusions or recommendations expressed in this material are those of the author(s) and do not necessarily reflect the views of the Under Secretary of Defense for Research and Engineering.

In order to tackle the aforementioned challenges, we recently developed a new class of O-PCMs, Ge-Sb-Se-Te (GSST) alloys. A series of GSST thin films with the compositions of $Ge_2Sb_2Se_xTe_{5-x}$ (x = 1, 2, 3, 4, and 5) were prepared using thermal evaporation. Figure 1(b-d) plot refractive index (n) and extinction coefficient (k) dispersions measured in the chalcogenide alloys with a varied Se-to-Te atomic ratio at its amorphous (**Error! Reference source not found.**b) and crystalline (**Error! Reference source not found.**c) states. **Error! Reference source not found.**d shows the calculated FOM of the alloys. Among the studied compositions, $Ge_2Sb_2Se_4Te_1$ (further in the text abbreviated as GSST) demonstrates the highest FOM~100, which stems from its large Δn of 1.2 – 1.5 across the near- to mid-IR bands while maintaining low optical loss at both structural states from 2 – 7 μm. The optical loss of GSST is two orders of magnitude lower than that of the classical phase change alloy GST-225. While Se doping in phase change alloys has been previously investigated, such exceptional optical behavior has not been studied.

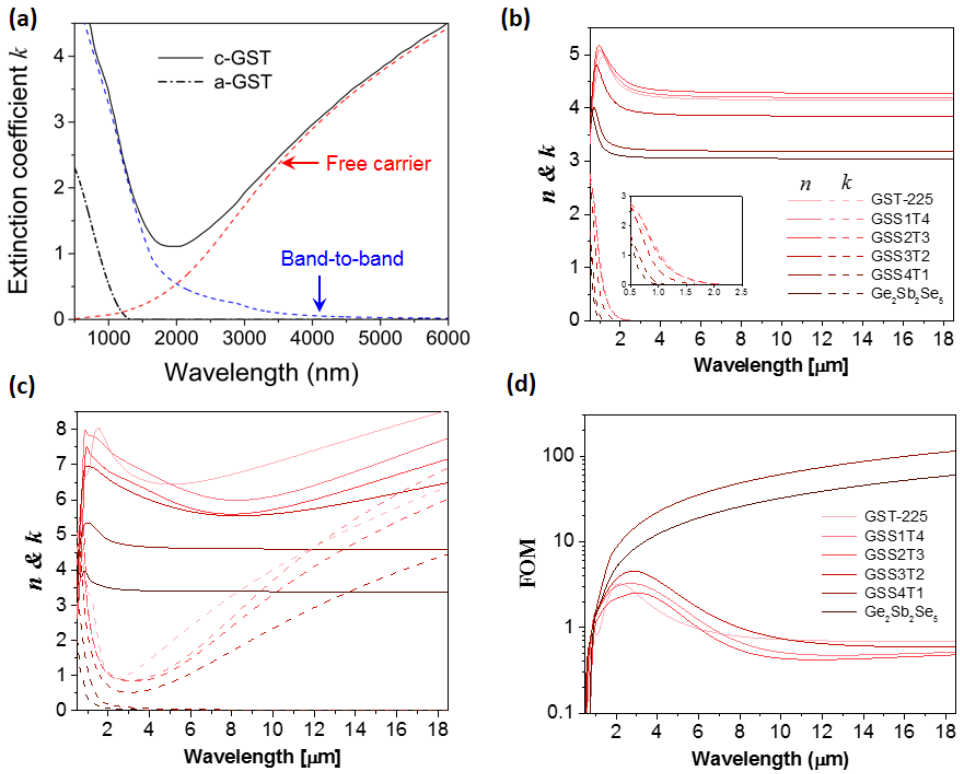

Figure 1. (a) Optical absorption of the classical phase change alloy $Ge_2Sb_2Te_5$ fitted to show combined contributions from interband transition, Urbach tail, and FCA based on Drude models. (b-d) Optical properties of $Ge_2Sb_2Se_xTe_{5-x}$ films. (b, c) Measured real (n) and imaginary (k) parts of refractive indices of the (b) amorphous and (c) crystalline alloys. (d) Material FOMs (Δn/k). Data from reference [9].

The remarkable low-loss performance benefits from blue-shifted interband transitions as well as minimal free-carrier absorption due to significantly reduced free carrier concentration and mobility. Our material design and choice is rationally guided by density functional theory computations, which allows prediction of the phase and electronic structures of alloys in the GSST family.

2. SWITCHING OF FREE-SPACE REFLECTIVE PIXEL

As a proof-of-concept demonstration of reconfigurable GSST-based free space devices, we constructed a pixel-level (30 × 30 μm^2) electrothermal non-volatile switching element for free-space reflection modulation. In the device, phase transition of a single-layer GSST film was reversibly actuated by joule heating, as illustrated in Fig. 2a. The heating was generated by a tungsten metal layer located under the GSST patch. Voltage pulses were applied to the micro-heater via the gate of a power MOSFET connected in series to the device. Fig. 2b shows the SEM image of a full device with the contact pads and Fig. 2c depicts the zoom-in view of the GSST-based pixel. The time dependent reflectance of the pixel was monitored with InGaAs video camera, frame rate was set to 100 fps. Fig. 2d demonstrates an absolute reflectance in the range from 24% to 34%, which corresponds to a relative change of 41%. The contrast can be improved with an optimized multilayer stack design. Raman spectra from Fig. 2e verify structural transformation of the material, more specifically, crystalline (120 cm^{-1}) and amorphous (160 cm^{-1}) peaks are observed after the corresponding actuation. The device can endure over 1000 reversible switching cycles without appreciable damage or degradation.

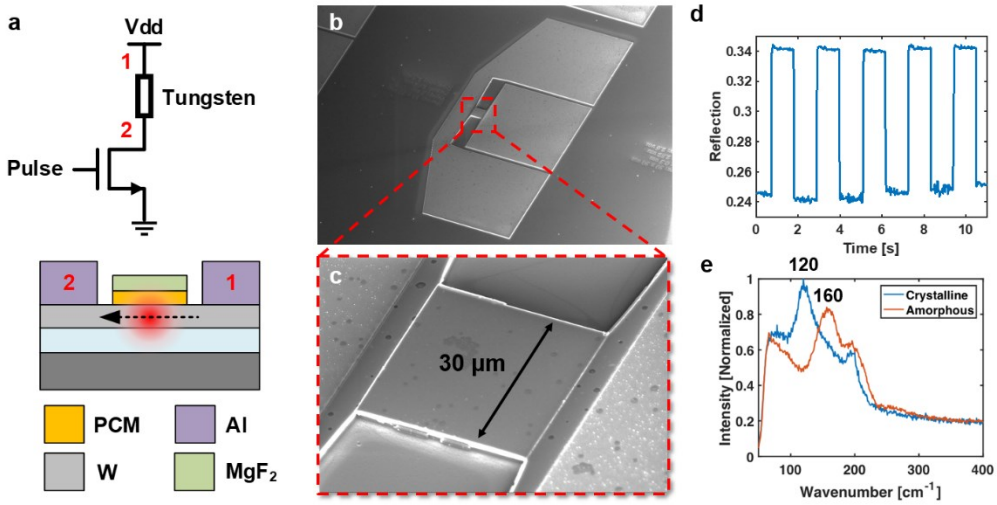

Figure 2. Electrothermally switchable pixel: (a) Schematic of the device and test setup. (b) SEM of the device used to switch a 30 μm × 30 μm pixel. (c) Zoom-in on the pixel with a square pattern of GSST. (d) Time-dependent absolute reflection measurements of a 1550 nm laser focused onto the pixel. (e) Raman measurements of the GSST film.

3. RECONFIGURABLE METALENS WITH A SWITCHABLE FOCUS

The mid-infrared is a frequency band strategically important for numerous biomedical, military, and industrial applications. Further development of mid-IR devices is hindered by the lack of inexpensive and efficient basic optical elements, such as lenses, wave plates, filters, etc. Furthermore, the available components are typically bulky and passive. Our research addresses these challenges by leveraging novel low-loss optical phase-change materials (GSST) and their sub-wavelength patterning to achieve ultra-thin (thickness < $\lambda_0/8$), high-efficiency (>40%), and multi-functional mid-IR components. As a proof-of-principle, we demonstrated a reconfigurable bifocal metalens with a switchable focus. We believe that our findings will enable new range of compact, multi-functional spectroscopic and thermal imaging devices.

Our metalens principle is based on collective Mie scattering of incident plane wave by subwavelength dielectric structures, which sustain both electric and magnetic dipolar resonances. Each of the scatterers, also known as Huygens' meta-atoms[10,11], contributes to the phase and amplitude of the incident beam. The amount of phase shift was controlled by the meta-atom geometry and its refractive index. Proper spatial arrangement of meta-atoms can reconstruct a desired phase profile. For instance, lens functionality can be achieved by introducing a hyperboloid phase distribution.

The metasurface operation concept is illustrated in Fig. 3a: in amorphous state (A-state) the lens focuses the incident light at a focal length of 1 mm and after the heating-induced material state transition the focal length changes to 1.5 mm (C-state). The switching of the focal length was attained by changing the hyperboloidal phase profiles shown in Fig. 3c. For

simplicity, we performed binary discretization of original continuous phase distributions: 0° phase shift – black, 180° – white. Then, we formed a library of four distinct meta-atoms which can realize the binary transitions. The metalens was fabricated by depositing a 1-μm-thick GSST film onto CaF_2 substrate followed by patterning processes involving electron-beam lithography patterning and reactive ion etching with a mixture of fluoromethane gases. Figure 3b depicts zoomed-in metasurface image obtained by SEM.

We characterized the GSST bifocal metalens by imaging its focal spot and measuring focusing efficiency by using custom-made optical setups. The incident beam with linear polarization and wavelength of 5.2 μm was generated by a quantum cascade laser. Then metalens produced a focal spot, which was further magnified about 70 times by a two-lens assembly and imaged with a mid-IR focal plane array. Figure 4a shows experimentally measured focus intensity distribution, which matches reasonably well with the theoretical point spread function (PSF) (see Fig. 4b,c) calculated by using Kirchhoff diffraction integral approach. From the data analysis, we retrieved that our metalens produces a diffraction limited focal spot with a Strehl ratio of 0.9, focal spot diameter of 10 μm, and depth of focus ±7 μm. The focusing efficiency, defined as the ratio of the focused laser power (power transmitted through a 200 μm pinhole) to the power incident on the metalens interface, was measured to be about 10-15%.

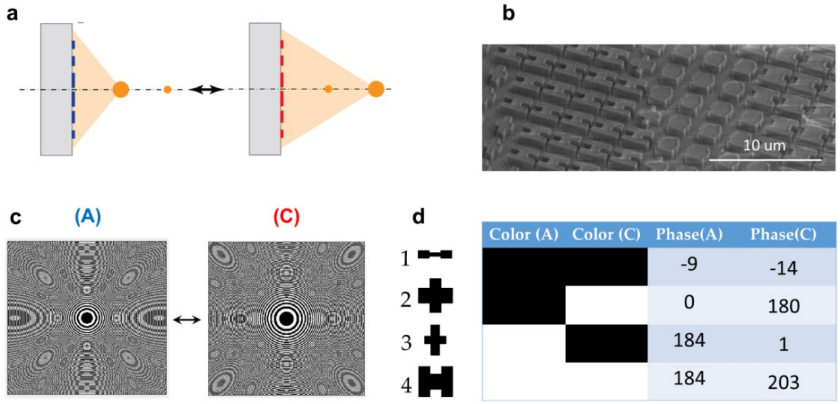

Figure 3. (a) Mid-IR bifocal reconfigurable metalens based on GSST: working principle, design, and fabrication. (a) Illustration of functionality concept: under GSST phase transition metalens switches the focal length from 1 mm in A-state (blue) to 1.5 mm in C-state (red); (b) SEM scan of the fabricated 1 bit metalens; (c) 1bit-discretized phase distribution for achieving focusing capability in A and C states; (d) library of meta-atoms used in phase-profile transformation Strehl ratio as a function of imaging plane position.

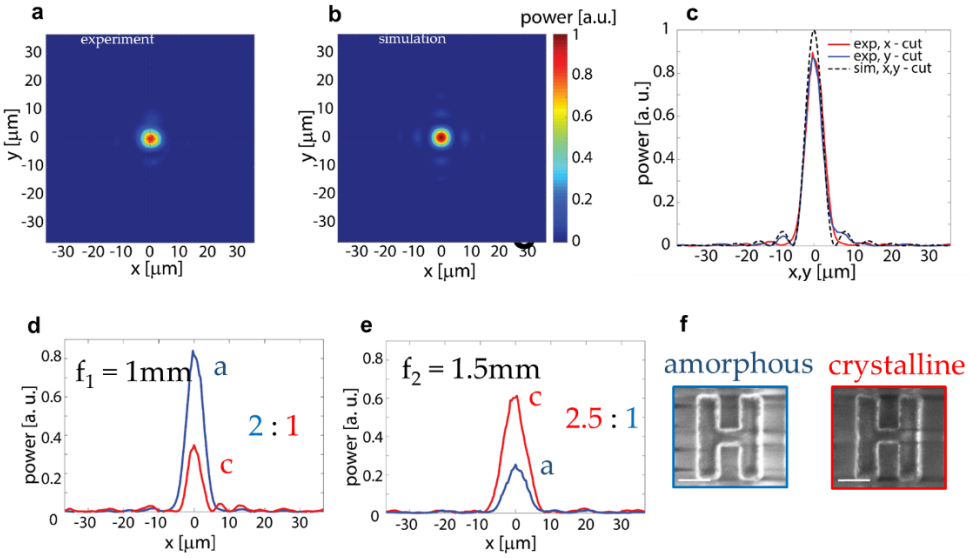

Figure 4. (a) Mid-IR bifocal reconfigurable metalens based on GSST: optical performance characterization, switching test. (a) Measured and (b) simulated power distribution of the focal spot produced by GSST metalens. (c) Focal spot cross-sections along x and y axes combined with the theoretically obtained PSF. Intensity profiles at the focal distance of $f_1 = 1$ (d) cm and $f_2 = 1.5$ cm (e). Blue and red curves indicate measurements with the metasurface in amorphous (a) and crystalline (c) states. (f) SEM scans verifying that the shape and dimensions of the meta-atoms were preserved during the amorphous-to-crystalline structural transformation.

To demonstrate the focal switching functionality, we annealed the metalens on a hot plate at 275°C for 30 minutes in argon atmosphere and then repeated the same focal spot imaging measurements. We observed that after annealing procedure, most of the power was focused at a distance f_2 = 1.5 cm (red curves in Fig. 4d,e) instead of f_1 = 1 cm for the untreated sample (blue curves in Fig. 4d,e). Hence, our 1-bit metalens performed bifocal switching with a contrast ratio of 5. With the help of SEM analysis, we confirmed that during material phase transition the meta-atoms shapes and dimensions remained unchanged (Fig. 4f), hence the focal switching performance was caused by the GSST refractive index change. In the future, the metalens performance can be further improved by more sophisticated designs based on multi-bit phase discretization and including into the designs more of fabrication-related nuances

4. NON-VOLATILE INTEGRATED PHOTONIC SWITCHES

An optical switch is a key component of dynamic integrated photonic circuitry. Conventionally, optical switches utilize electro-optic or thermo-optic phenomena, which introduce a tiny change in the optical properties and hence require the devices to be exceedingly long. In contrast, optical phase-change materials (O-PCM), such as GST-225, can provide large index contrast, which is instrumental in significantly reducing the device foot print. However, at telecom wavelengths, GST-225 exhibits high losses, which lead to relatively low FOMs of 2.0 and 0.4[12], respectively. As a result, the optical switches based on these materials demonstrated moderate performance quantified by contrast ratio (CR) of 12 dB and insertion loss (IL) of -2.5 dB[13]. Additionally, crosstalk and parasitic losses in these devices hamper their scalable integration and implementation of large-scale, functional photonic circuits. In this work, we employed exceptional optical properties of the newly developed GSST to realize a non-volatile optical switch with a superior performance.

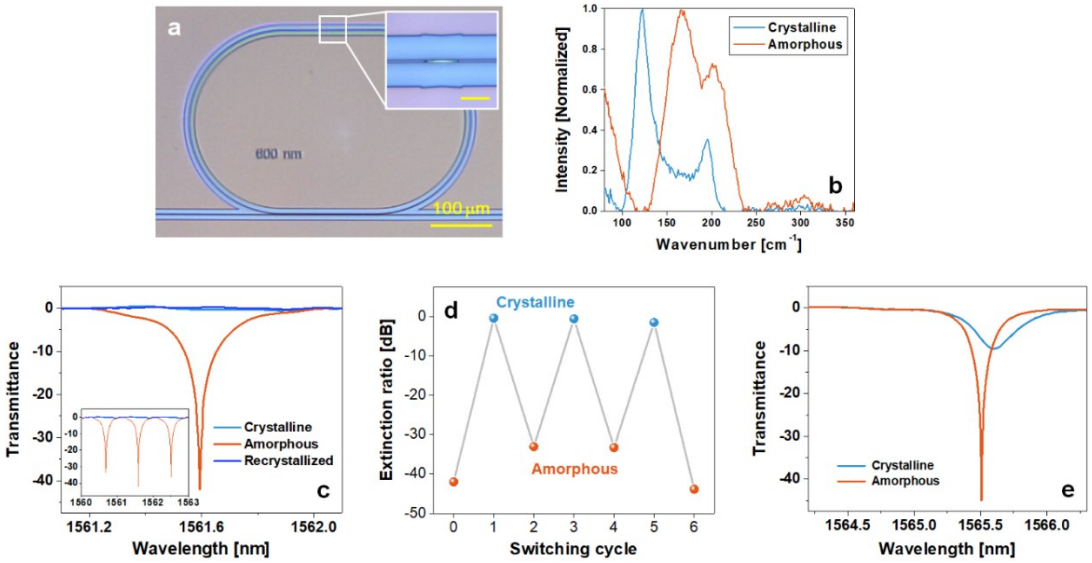

Figure 5. (a) Mid-IR bifocal reconfigurable metalens based on GSST: optical performance characterization, switching test. (a) Measured and (b) simulated power distribution of the focal spot produced by GSST metalens. (c) Focal spot cross-sections along x and y axes combined with the theoretically obtained PSF. Intensity profiles at the focal distance of f_1 = 1 cm (d) and f_2 = 1.5 cm (e). Blue and red curves indicate measurements with the metasurface in amorphous (a) and crystalline (c) states. (f) SEM scans verifying that the shape and dimensions of the meta-atoms were preserved during the amorphous-to-crystalline structural transformation.

First we demonstrate a narrow band photonic switch: a SiN racetrack resonator coupled to a bus waveguide. Optical image of the structure is shown in Figure 5a. We deposited a 50-nm thick strip of GSST on top of the resonator as depicted in the inset to Figure 5a. Phase transition of GSST was controlled by laser-induced heating and probed via Raman spectroscopy. Raman spectra were collected from the GSST strip in both structural states, peaks at 160 cm^{-1} and 120 cm^{-1} are the signatures of the amorphous and crystalline phases, respectively (Fig. 5b). In order to confirm switching reversibility, we

performed a crystallization-reamorphization-recrystallization cycle and observed a reasonable match between the transmission spectra of the initial crystalline and recrystallized states, depicted with light blue and blue curves in Fig. 5c.

Afterwards, the test on reversible on/off switching was repeated a couple of times and the device demonstrated successful reproducible optical response evidenced by extinction ratio data in Fig. 5d. The device also exhibited a large switching CR of 42 dB and a low IL of < 0.5 dB, far outperforming previous non-volatile switches[13]. Such remarkable performance was supported by the theoretical studies based on the measured optical constants (Fig. 1) and was attributed to its exceptional FOM. As a reference, we fabricated and characterized a similar device with a strip made of conventional GST-225 instead of GSST. Figure 5e shows that the reference device in the "off" state still had a transmittance dip, i.e. the strip did not completely turn off even when GST-225 was transformed into crystalline state.

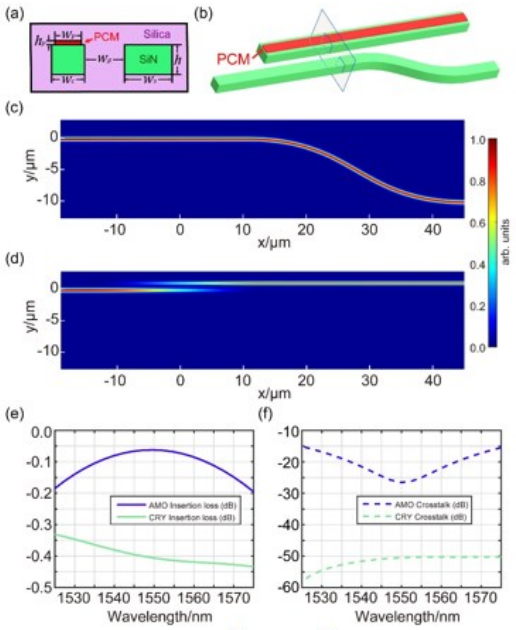

Figure 6

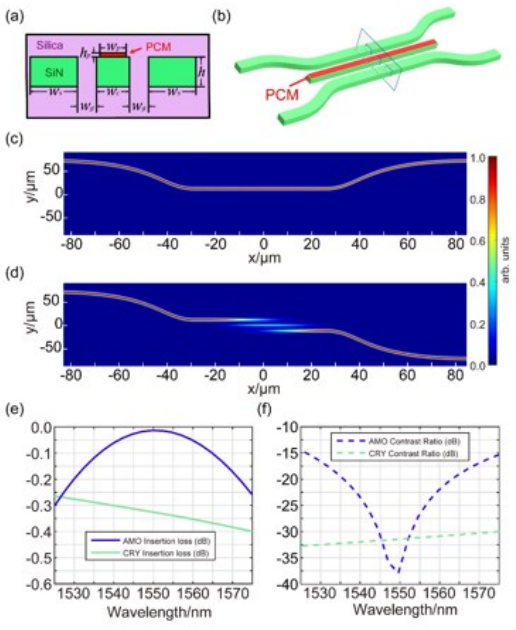

Figure 7

Figure 6&7. (a, b) Cross section and 3D schematics of the waveguide structures. (c, d) Optical intensity distributions. (e, f) Insertion loss and crosstalk of the designed 1 by 2 and 2 by 2 photonic switches.

Next, we report the design and modeling of a new kind of broadband photonic switches combining low-loss phase change alloys and a "nonperturbative" design to boost the switching performance. Switches based on classical O-PCMs, whether theoretically analyzed[14,15] or experimentally implemented[1,13,16], exhibit unoptimized performance with high ILs of 2 dB or more and limited crosstalk of less than 15 dB in the C-band. In our design, on the one hand, we use the low-loss O-PCM for this application: GSST. On the other hand, the switch design is based on the huge index change of O-PCMs. The basic element is a directional coupler comprised of a bare waveguide (WG1) and a waveguide covered with a PCM strip (WG2). At (a-) state, their indices are matched, and light will be coupler from WG1 to WG2. At (c-) state, due to the large index change of O-PCM, the modal profile will be completely different, and effective index of WG2 will increase a lot so that coupling will not happen. This helps to keep the loss at a low level since light will not travel in WG2 when GSS4T1 is in its (c-) state. Fig 6 and 7 show the state-of-the-art performance of the 1 by 2 and 2 by 2 switches designed by this method. The switches demonstrate significantly enhanced performances compared to current state-of-the-art. Across the telecom C-band, individual 1 × 2 and 2 × 2 switches exhibit ILs between 0.01 to 0.4 dB, and CTs consistently above 15 dB (> 25 dB at 1550 nm)[17]. We have also proven that even better switching performance is possible with a dual-etch design, with center waveguide having a different than the other two waveguides: a representative example for the compact 15.4 μm coupling length is an IL(Cross) of -0.048 dB with CT lower than 38.1 dB over the 70-nm -0.3dB-IL bandwidth[18].

5. SUMMARY

In the scope of this work, we developed a new class of O-PCMs engineered to achieve index-only modulation free from the loss penalty. GSST demonstrates unprecedented material FOM over two orders of magnitude larger than that of classical GST alloys, benefiting from blue-shifted interband transitions as well as minimal free carrier absorption. Based on its phase-change capabilities, we implemented a reconfigurable bifocal metalens and demonstrated its focal length switching with a contrast ratio of 5 and focusing efficiency larger than 10%. In addition, we realized a narrowband nonvolatile optical switch with a contrast ratio of 42 dB and insertion loss below 0.5 dB and proposed a nonperturbative design method for directional coupler based switches with record low loss and switching contrast. These state-of-the-art performances, derived from the exceptional FOM of the material, qualify the device as useful building blocks for scalable photonic networks. Finally, an electrothermally switched free-space reflective pixel was demonstrated with a microsecond amorphization switching time and relative contrast of 41% at 1550 nm. These results enable a new path for optical and electrical infrared light control for both free-space and integrated photonics applications, such as tunable metasurfaces, spatial light modulators, tunable spectral filters, subwavelength reflective phased arrays, beam steering, and holography.

ACKNOWLEDGEMENTS

This material is based upon work supported by the Assistant Secretary of Defense for Research and Engineering under Air Force Contract No. FA8721-05-C-0002 and/or FA8702-15-D-0001, and by the Defense Advanced Research Projects Agency Defense Sciences Office (DSO) Program: EXTREME Optics and Imaging (EXTREME) under Agreement No. HR00111720029. The authors also acknowledge characterization facility support provided by the Materials Research Laboratory at MIT, as well as fabrication facility support by the Microsystems Technology Laboratories at MIT and Harvard University Center for Nanoscale Systems. The views, opinions and/or findings expressed are those of the authors and should not be interpreted as representing the official views or policies of the Department of Defense or the U.S. Government.

REFERENCES

[1] M. Rudé, J. Pello, R. E. Simpson, J. Osmond, G. Roelkens, J. J. van der Tol, and V. Pruneri, "Optical switching at 1.55 μm in silicon racetrack resonators using phase change materials," Appl Phys Lett **103**, 141119 (2013).

[2] Q. Wang, E. T. F. Rogers, B. Gholipour, C. M. Wang, G. H. Yuan, J. H. Teng, and N. I. Zheludev, "Optically reconfigurable metasurfaces and photonic devices based on phase change materials," Nat Photonics **10**, 60-65 (2016).

[3] C. Ríos, M. Stegmaier, P. Hosseini, D. Wang, T. Scherer, C. D. Wright, H. Bhaskaran, and W. H. Pernice, "Integrated all-photonic non-volatile multi-level memory," Nat Photonics **9**, 725-732 (2015).

[4] P. Hosseini, C. D. Wright, and H. Bhaskaran, "An optoelectronic framework enabled by low-dimensional phase-change films," Nature **511**, 206-211 (2014).

[5] A.-K. U. Michel, D. N. Chigrin, T. W. Maß, K. Schönauer, M. Salinga, M. Wuttig, and T. Taubner, "Using low-loss phase-change materials for mid-infrared antenna resonance tuning," Nano Lett **13**, 3470-3475 (2013).

[6] X. Y. Sun, Q. Du, T. Goto, M. C. Onbasli, D. H. Kim, N. M. Aimon, J. Hu, and C. A. Ross, "Single-step deposition of cerium-substituted yttrium iron garnet for monolithic on-chip optical isolation," ACS Photonics **2**, 856-863 (2015).

[7] J. -L. Adam, X. Zhang, "Chalcogenide glasses: preparation, properties and applications," (Woodhead publishing, 2014).

[8] Lyeo, H.K., Cahill, D.G., Lee, B.S., Abelson, J.R., Kwon, M.H., Kim, K.B., Bishop, S.G. and Cheong, B.K., 2006. "Thermal conductivity of phase-change material $Ge_2Sb_2Te_5$," Appl Phys Lett, **89**, 151904 (2006).

[9] Y. Zhang, J. B. Chou, J. Li, H. Li, Q. Du, A. Yadav, S. Zhou, M. Y. Shalaginov, Z. Fang, H. Zhong, C. Roberts, P. Robinson, B. Bohlin, C. Ríos, H. Lin, M. Kang, T. Gu, J. Warner, V. Liberman, K. Richardson and J. Hu, "Extreme Broadband Transparent Optical Phase Change Materials for High-Performance Nonvolatile Photonics," arXiv preprint arXiv:1811.00526 (2018).

[10] C. Pfeiffer and A. Grbic, "Metamaterial Huygens' Surfaces: Tailoring Wave Fronts with Reflectionless Sheets," Phys. Rev. Lett. **110**, 197401 (2013).

[11] L. Zhang, J. Ding, H. Zheng, S. An, H. Lin, B. Zheng, Q. Du, G. Yin, J. Michon, Y. Zhang, Z. Fang, M. Y. Shalaginov, L. Deng, T. Gu, H. Zhang, and J. Hu, "Ultra-thin high-efficiency mid-infrared transmissive Huygens meta-optics," Nat. Commun. **9**, 1481 (2018).

[12] B.-S. Lee, J. R. Abelson, S. G. Bishop, D.-H. Kang, B.-k. Cheong, and K.-B. Kim, "Investigation of the optical and electronic properties of $Ge_2Sb_2Te_5$ phase change material in its amorphous, cubic, and hexagonal phases," J. Appl. Phys. **97**, 093509 (2005)

[13] M. Stegmaier, C. Ríos, H. Bhaskaran, C. D. Wright, and W. H. P. Pernice, "Nonvolatile All-Optical 1 × 2 Switch for Chipscale Photonic Networks," Adv. Opt. Mater. **5**, 2–7 (2017).
[14] Y. Ikuma, T. Saiki, and H. Tsuda, "Proposal of a small self-holding 2× 2 optical switch using phase-change material," IEICE Electronics Express **5**, 442-445 (2008).
[15] H. Liang, R. Soref, J. Mu, A. Majumdar, X. Li, and W.-P. Huang, "Simulations of Silicon-on-Insulator Channel-Waveguide Electrooptical 2× 2 Switches and 1× 1 Modulators Using a $Ge_2Sb_2Te_5$ Self-Holding Layer," J. Lightwave Technol. **33**, 1805-1813 (2015).
[16] T. Moriyama, D. Tanaka, P. Jain, H. Kawashima, M. Kuwahara, X. Wang, and H. Tsuda, IEICE Electronics Express **11**, 20140538-20140538 (2014).
[17] Q. Zhang, Y. Zhang, J. Li, R. Soref, T. Gu, J. Hu, "Broadband Nonvolatile Photonic Switching Based on Optical Phase Change Materials: Beyond the Classical Figure of-Merit," Optics Letts., **43,** 94-97 (2018).
[18] F. De Leonardis, R. Soref, V. M. N. Passaro, Y. Zhang, and J. Hu, "Broadband electro-optical crossbar switches using low-loss $Ge_2Sb_2Se_4Te_1$ phase change material," *J. Lightwave Technol.* (2019). DOI: 10.1109/JLT.2019.2912669